Fast and Reliable Human Exposure Assessment Around High Power Systems Using Surrogate Modeling

IEEE Access
Multidisciplinary ⋮ Rapid Review ⋮ Open Access Journal

Received 15 January 2024, accepted 29 January 2024, date of publication 16 February 2024, date of current version 8 March 2024.

Digital Object Identifier 10.1109/ACCESS.2024.3366654

RESEARCH ARTICLE

Fast and Reliable Human Exposure Assessment Around High Power Systems Using Surrogate Modeling

PAUL LAGOUANELLE[1,2], FABIO FRESCHI[1,3], (Senior Member, IEEE), LIONEL PICHON[2], AND LUCA GIACCONE[1], (Senior Member, IEEE)

[1]Dipartimento Energia "G. Ferraris," Politecnico di Torino, 10129 Turin, Italy
[2]Group of Electrical Engineering–Paris (GeePs), UMR CNRS 8507, CentraleSupélec, Université Paris-Saclay, Sorbonne Université, 91192 Gif-sur-Yvette, France
[3]School of Information Technology and Electrical Engineering, University of Queensland, Brisbane, QLD 4072, Australia

Corresponding author: Paul Lagouanelle (paul.lagouanelle@latmos.ipsl.fr)

ABSTRACT Due to the high level of magnetic stray field around high power electromagnetic systems, the human exposure needs to be properly assessed in order to check the compliance with international standards and guidelines. Such analyses are usually made in two steps: first a proper map of the magnetic field in the vicinity area is computed, where, in a second time a human model is used to compute induced dosimetric quantities. Unfortunately, such high power systems have a high computational cost in addition to the complexity of 3D human models. Thus, this paper shows the useful combination of stochastic tools with numerical solvers in order to build accurate predictors at a low computation cost in the case of human exposure for various high power systems. These surrogate models can be used to accurately analyze the sensitivity of the exposure problem regarding various input parameters at a low computation cost. A dosimetric methodology for assessing the safety of a human body around an inductive power transfer system for automotive applications, using an adaptive metamodelling algorithm coupled with a voxelized 3D human model, has been developed. Such analysis has been successfully extended to a system where human exposure assessment are crucially needed: medium-frequency direct-current welding guns, treating the case of human exposure to a pulsed magnetic field. This methodology manages to reduce the computation time by more than 99.9% compared to a classical analysis for both exposure problems.

INDEX TERMS Human exposure, stochastic methods, numerical dosimetry, metamodel, wireless power transfer, spot welding.

I. INTRODUCTION

Wireless power transfer (WPT) systems are a key factor in the development of electric mobility for the near future. Such systems implies a high level of magnetic stray field which exceed limits for occupational and general public exposure [1]. Therefore, when designing new systems, a great care should be taken when evaluating the level of exposure in order to be compliant with the relevant standards and guidelines [2], [3] for human exposure. Moreover, in the industry, a wider range of high-power systems are present and need proper human exposure assessment, such as medium-frequency direct-current (MFDC) welding applications also investigated here.

To properly assess human exposure issues near a high power system, some proper modeling tools have to be developed. Usually for the aforementioned industrial applications, such analyses are made in two steps: first, the magnetic field is mapped on a defined area, then, a voxelized 3D human model is placed in the Magnetic Flux density in order to compute the induced electric field within the human body. For the Duke's model [4] considered here, the resolution can go down to 0.5 mm × 0.5 mm × 0.5 mm. Thus, the computation grid is usually made of over 10 million cells depending on the posture. Moreover, due to the complexity of most high power industrial devices, in order to perform an accurate sensitivity analysis on the human exposure

The associate editor coordinating the review of this manuscript and approving it for publication was Ladislau Matekovits.

(regarding the variations of several input parameters), several accurate mappings of the magnetic field would require too many calls of the computational model. Thus, the computation for the assessment of human exposure cannot use only 3D solvers, which would take too much time. For the computation of human exposure to high power systems, many computational methods have been recently developed which aim at reducing computation time. For automotive applications, Yavolovskaya et al. developed an adapted method of moments using volume integral equations to bypass the use of heavy computational methods such as FDTD or FEM [5]. Using two-step scaled-frequency FDTD methods for an inductive power transfer system, Zang et al. managed to reduce their computation time by two thirds [6]. For voxelized human models, a great interest is to explore different postures, for example in [7], the source terms are deformed in order to use a non-postured body model to compute the exposure of a given posture. In [8], by assigning an impedance at each edge of each voxel, the induced E-field can be easily computed in a complete realistic 3D human model. Finally, in the case of pulsed magnetic fields (such as MFDC welding guns), the Scalar-Potential Finite-Differences (SPFD) method [9] has already been used successfully for computing induced current densities in the human body [10].

A possible alternative approach is to combine the available solvers with some non-intrusive stochastic algorithms to save a great amount of computation time by building a metamodel: given an input dataset, a metamodel which interpolates the real model given by the 3D solver can be built. This metamodel is simply a mathematical function which can be used instead of the real model to compute huge amount of datapoints at a low computation cost. This makes it possible to deal with the variability of all the parameters describing the electromagnetic problem. Such surrogate models and especially Polynomial Chaos expansion (PCE) and Kriging methods have already been successfully used for the exposure of a fetus to RF electromagnetic fields [11] or for the determination of reference levels due to a WPT system [12]. This paper shows that such an approach coupled with an adaptive sampling algorithm is particularly well suited for a dosimetric analysis for a high power system where the whole human body needs to be considered.

II. SURROGATE MODEL

A. HUMAN EXPOSURE ASSESSMENT

The direct model considered here for the computation of human exposure assessment consists in a classical two-step analysis: first, the distribution of the magnetic field is computed in a defined volume, then, the induced electric field within the human body is computed.

For both exposure problems presented here, the investigated frequencies are falling in the low frequency range: $f = 85\,\text{kHz}$ in section III and $f < 5\,\text{kHz}$ in section IV. This enables us to simply the first electromagnetic problem by assuming that the induced currents in the body are negligible regarding the current source [13]. Therefore, the magnetic field distribution is not modified by induced currents and can be computed independently of the conducting body. This computation can be made by any solver: a specific Boundary Element Method solver for the WPT case [14] or a classical FDTD Low-Frequency solver using the Sim4Life software from SPEAG [4] for the MFDC spot welding gun case.

In a second step, once the magnetic field distribution along with its corresponding magnetic vector potential is known in the investigation volume. The induced electric potential in a 3D human body is computed using the Scalar-Potential Finite Difference Method [15] from the Magneto Quasi-Static Solver in Sim4Life. The solution equation within a voxel with the quasi-static approximation can be written as followed [16]:

$$\nabla \cdot \left((\sigma + \mathrm{j}\omega\varepsilon_r\varepsilon_0)\, \nabla\varphi \right) = -\mathrm{j}\omega \nabla \cdot \left((\sigma + \mathrm{j}\omega\varepsilon_r\varepsilon_0)\, \mathbf{A_0} \right) \quad (1)$$

where φ is the induced electric potential, $\mathbf{A_0}$ the magneto-static vector potential, and ω the angular frequency. The dielectric properties of the tissue at the angular frequency ω are noted by σ, the tissue conductivity, and ε_r its relative permittivity, which both varies with the frequency [17]. As the magnetic field has been supposed independent from the conducting body, the source term $\mathbf{A_0}$ in equation 1 is fully known from the previous step. This equation can be solved to obtain the electric potential and by integration the induced electric field in the targeted voxel.

B. PCK METAMODEL

Polynomial Chaos-Kriging (PCK) metamodelling combines both PCE and Kriging to build an exact interpolator of an output model $\mathcal{M}(\boldsymbol{x})$. Kriging is used to interpolate the local variations of the output model while PCE is useful for the global approximation. A PCK metamodel is defined by [18]:

$$\widehat{\mathcal{M}}(\boldsymbol{x}) = \sum_{\boldsymbol{\alpha}\in\mathcal{A}} y_{\boldsymbol{\alpha}}\, \psi_{\boldsymbol{\alpha}}(\boldsymbol{x}) + \sigma^2 Z(\boldsymbol{x}, \omega) \quad (2)$$

where $\sum_{\boldsymbol{\alpha}\in\mathcal{A}} y_{\boldsymbol{\alpha}}\, \psi_{\boldsymbol{\alpha}}(\boldsymbol{x})$ is a weighted sum of orthonormal polynomials describing the trend of the PCK model, σ^2 and $Z(\boldsymbol{x}, \omega)$ denote the variance and the zero mean, unit variance, stationary Gaussian process, respectively. This metamodel will be used to build a predictor of the heavy computational direct model previously presented for human exposure assessment.

Based on various prior analysis discussed in [19], the Matérn-5/2 covariance function along with a Legendre polynomial basis gave the best results in terms of accuracy of our PCK metamodel. Similarly, a maximum polynomial degree of 10 has been chosen in order to avoid useless time-consuming computations. All the development made on the surrogate models in this article have been made in the case of frequencies falling in the low frequency range only. For higher frequencies problems, these base parameters would have to be changed and therefore various prior analysis on simple higher frequency systems are required.

C. A POSTERIORI ERROR ESTIMATION

In order to greatly reduce the number of computed input datapoints, the aforementioned surrogate process has been coupled with an active learning sampling method based on the quad-tree algorithm [20] with a defined consistency metric. Starting from a low number of samples and thus an inaccurate metamodel, the algorithm is enriching sequentially the training dataset in the regions of interest (where the consistency of the metamodel is the lowest), in order to build an accurate metamodel [21].

Let us consider a training set $\{(\boldsymbol{x}_1, \boldsymbol{y}_1), \ldots, (\boldsymbol{x}_n, \boldsymbol{y}_n)\}$ of n various input datapoints and their corresponding outputs. The consistency of the metamodel is calculated using the mean Leave-One-Out error (LOO):

$$LOO = \frac{1}{n}\sum_{i=1}^{n}\left(\frac{||\widehat{\mathcal{M}}_{/i}(\boldsymbol{x}_i) - \boldsymbol{y}_i||}{||\boldsymbol{y}_i||}\right)^2 \tag{3}$$

where $\widehat{\mathcal{M}}_{/i}$ is the metamodel that was trained using all $(\boldsymbol{x}, \boldsymbol{y})$ but $(\boldsymbol{x}_i, \boldsymbol{y}_i)$. The LOO enables us to evaluate the consistency of the metamodel considering its build. If the LOO is close to 1, the predictor is highly inaccurate outside of the training dataset, whereas the smallest it is, the more accurate the predictor is, outside of the training dataset.

Many other metrics can be used such as the k-fold or RMSE. But the LOO does not require additional calls of the input model, thus, saving a lot of computation time for an expensive computational model. Moreover as the main goal of this work is to perform sensitivity analysis and draw tendencies for the field exposure, the constraints on the safety areas around the considered devices do not impose heavy accuracy of our predictors. Therefore, given the dimensionality and the size of the training datasets used for the systems considered here, the LOO represents a good compromise as it is extremely fast to compute for a low number of input samples while being an excellent quality tracker for low dimensionalities [22].

Although, for higher dimensionalities and bigger number of samples, the LOO is not suited anymore, and a proper analysis with a new definition of an adapted quality tracker is required. A possibility is to compute a validation set uncorrelated with the training dataset on which the maximum error for the predictor could be computed. Additional developments can be found here [19].

D. SENSITIVITY ANALYSIS

One of the main advantages of building a consistent surrogate model for the expensive computational model with only a handful of training samples $n_{samples}$, is that many datapoints can be computed at a low computation cost for mapping areas or performing accurate sensitivity analysis. For the following models, our sensitivity trackers are the variance-based Sobol' indices [23]:

$$S_P = \frac{Var[\mathbb{E}[Y|P]]}{Var[Y]} \tag{4}$$

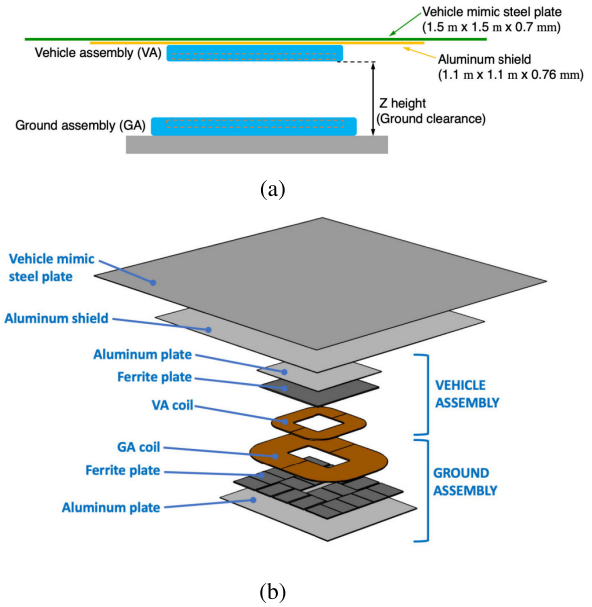

FIGURE 1. Cut plane (a) and 3D view (b) of the WPT3 (class Z3) system taken from from the SAE J2954 standard [25].

where Y is an output of the model and P a given parameter. Considering the variation of several input parameters at once: if $S_P \sim 1$, Y is highly dependent on P, whereas if $S_P \ll 1$, P has almost no influence on Y. The definition of this first order index S_P can be extended to higher interaction orders between parameters similarly. For the following sensitivity analysis, the total-order index S_P^T will be considered which takes into account all interaction orders for the given parameter P [24].

III. EXPOSURE TO A STANDARD WPT CHARGER

A. THE WPT3 (CLASS Z3) SYSTEM

Firstly, the exposure to a typical WPT charger has been assessed: the WPT3 (11.1 kV A at 85 kHz) class Z3 (Z height $\in$ [170 mm, 250 mm]) from the SAE J2954 standard [25] displayed in Fig. 1. The dimensions of the WPT system are detailed in table 1 along with the electromagnetic properties of the ferrites used in the design in table 2. The ferrite layers in the Ground Assembly are constructed of ferrite tiles of dimensions 100 mm $\times$ 150 mm $\times$ 5 mm and 100 mm $\times$ 100 mm $\times$ 5 mm.

In order to assess the worst case scenario in term of exposure, the car body is not modelled to avoid any shielding effect. Moreover, the WPT system has been modelled with the maximum misalignment allowed by the standard between the receiving and transmitting coils ($\Delta x = 75$ mm, $\Delta y = 100$ mm, $\Delta z = 250$ mm), thus creating a high level of magnetic flux density in the surrounding area exceeding the reference levels.

The magnetic vector potential for this system has been computed using a hybrid method coupling the surface impedance boundary conditions with the boundary element method [14]. It has been computed only in a vicinity volume (see Fig. 2), where x is the direction of motion for the car, y is the orthogonal direction and z the gravity axis.

TABLE 1. Dimensions of the vehicle and ground assembly from the SAE J2954 standard [25]: length (L), width (W) and height (H) in millimeters.

	Coil and Ferrite Only	Housing
Vehicle Assembly L x W x H	334 × 334 × 12.6	350 × 350 × 20
Ground Assembly L x W x H	650 × 510 × 21.5	750 × 600 × 60

TABLE 2. Ferrite material used in the vehicle and ground assembly from the SAE J2954 standard [25].

Material	MnZn
Initial Permeability (25 °C)	> 1000
Flux Density, B_S (100 °C) ($H = 1200\,\mathrm{A\,m^{-1}}$, 10 kHz)	> 400 mT
Core Loss, P_V (100 kHz, 200 mT, 100 °C)	$< 350\,\mathrm{kW\,m^{-3}}$

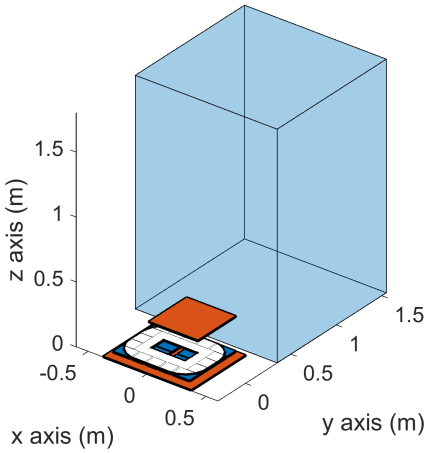

FIGURE 2. WPT3/Z3 system model from SAE J2954 (maximum misalignment between the coils) with an investigation volume (blue box of 1.2 m × 1.2 m × 1.8 m along the *x*, *y* and *z* axis).

B. POSTURE ANALYSIS

Based on already analyzed exposure situations in the literature [26], [27], using the unperturbed source field computed in the vicinity volume, the goal has been to try various realistic postures for the human body around this WPT charger. The FDTD Low-Frequency Magneto Quasi-Static solver has been used to compute the induced E-field in the whole body and inside the pelvis area, which is known to be extremely sensible to electromagnetic fields [9]. The model resolution has been set to 2 mm × 2 mm × 2 mm and three different postures (displayed in Fig. 3) have been investigated in this analysis and placed within the investigation volume (considered as vacuum):

- standing posture for the human body aside the charger, the normal position for a bystander;
- crouching on the side of the charger, which embodies for example an operator working on the car while it is charging;
- standing posture but bent over with hands opened towards the car, like someone ready to open one of the doors.

The choices for the investigated postures is purely arbitrary and could have been made differently but these postures made the most sense for us regarding possible situations of a practical WPT system.

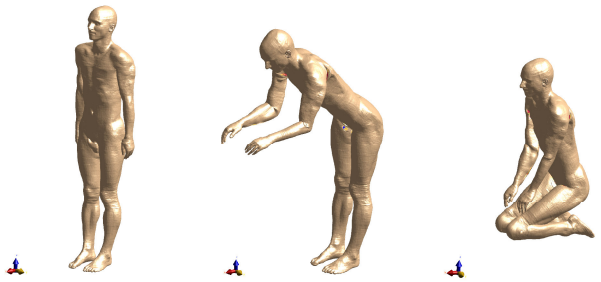

FIGURE 3. Investigated positions for the human exposure around the WPT3 (class Z3) charger displayed with Sim4Life: standing posture (a), bent over posture (b) and crouching posture (c).

TABLE 3. Maximum, 99$^{\mathrm{th}}$ percentile and average induced *E*-fields (V m^{-1}) in the whole body and the pelvis area along with the nearest distance to the system for the three studied postures exposed to the WPT3/Z3 charger.

	posture	max E	99$^{\mathrm{th}}$ E	$< E >$	distance
Whole body	standing	3.66	0.54	0.015	60 cm
	bent over	0.59	0.58	0.0033	54 cm
	crouching	6.07	0.68	0.012	15 cm
Pelvis	standing	3.59	0.42	0.033	81 cm
	bent over	0.16	0.10	0.16	96 cm
	crouching	1.09	0.52	0.032	60 cm

The maximum, 99$^{\mathrm{th}}$ percentile and average induced E-fields in the whole body and the pelvis area for the three studied postures exposed to the WPT3/Z3 charger are displayed on Table 3. For the induced E-field in the whole body, the 99$^{\mathrm{th}}$ percentile is the highest for the crouching posture next to the WPT charger. The average E-fields are logically similar for the standing position and the crouching position, while the bent over position has a lower one as some part of the human body are further from the charger compared to the other two positions. This is also the reason why the maximum E-field value in this case is close to the 99$^{\mathrm{th}}$ percentile value. The same analysis can be made for the critical pelvis area, where the crouching position seems the worst. In this case the difference in terms of 99$^{\mathrm{th}}$ percentile E-field value is even greater. Therefore for the remaining posture analysis, the crouching posture will be the one further investigated.

C. CHOICE OF AN EXPOSURE FACTOR

According to the ICNIRP guidelines [2], for a specific tissue i, the 99$^{\mathrm{th}}$ percentile E-field ($E^i_{99^{\mathrm{th}}}$) is the relevant value to compare with the restrictions in terms of exposure. Given a frequency value (e.g. 85 kHz) and using the reference levels provided by the ICNIRP, an exposure index EI^i can be defined for each tissue i within the human body:

$$EI^i = \frac{E^i_{99^{\mathrm{th}}}}{E^i_{lim}} \tag{5}$$

where E^i_{lim} is the basic restriction for general public exposure for the induced E-field in tissue i at the given frequency.

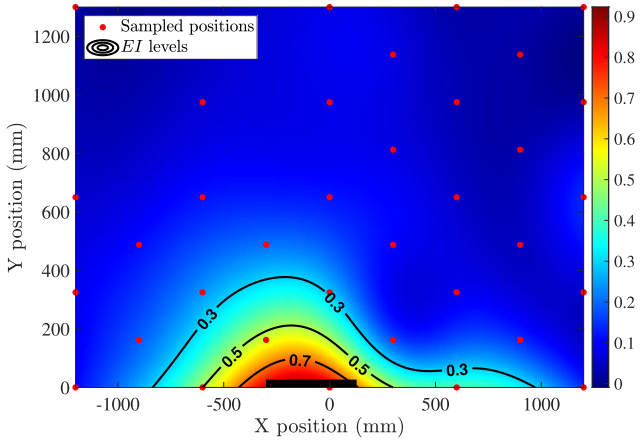

FIGURE 4. PCK metamodel ($n_{samples} = 35$, $LOO = 0.1945$) of $EI_{\max}(x, y)$ for various positions of a crouched operator around the WPT3/Z3 system (black rectangle).

It is worth noting that the 99$^{\text{th}}$ percentile E-field recommended by the ICNIRP can cause underestimation of the case of localised exposure [1], [28], [29], [30]. However, in this paper the attention is mainly focused on the method used to perform the exposure assessment. The proposed model performance is independent of the metric used to remove numerical artifacts. Therefore, in order to provide results compliant with the ICNIRP guidelines, we adopted the standard output provided by Sim4Life that is the 99$^{\text{th}}$ percentile E-field.

For quantifying the safety of a position (x, y) regarding the WPT system, the chosen exposure criteria is the maximum among all exposure indices available: $EI_{\max} = \max\left(\{EI^i, \forall i \text{ tissue}\}\right)$. When this value exceeds the unity, the basic restrictions are violated in at least one part of the human body, thus, the given position is not compliant with the standard. The goal of the analysis is to build a consistent predictor for $EI_{\max}(x, y)$ using the aforementioned adaptive surrogate modelling, which could then be used to define a safety area around the WPT system.

D. SAFETY AREA AROUND THE WPT SYSTEM

The active learning metamodelling algorithm has been used to compute a predictor for $EI_{\max}(x, y)$ around the WPT3/Z3 system. The resulting metamodel needed only $n_{samples} = 35$ with a consistency of $LOO = 0.1945$. The result is shown in Fig. 4 by means of a color map. Different levels for the exposure index ($EI_{\max} = [0.3, 0.5, 0.7]$) are also shown.

The analysis of Fig. 4 shows that there is no need to define a safety area for the operator around the WPT system as even close to the device the exposure index does not exceed 0.9. Moreover, when looking at the contour levels in Fig. 4, inside the main part of the investigation volume the exposure index does not exceed 30%. Since the coil misalignment is the greatest, and the posture leading to the worst exposure scenario has been considered, it can be assumed that the WPT3/Z3 device is compliant for all postures presented in this paper.

E. SENSITIVITY ANALYSIS AND DISCUSSION

A Sobol'-based sensitivity analysis with respect to the x and y position of the human body has been carried out. The following sensitivity indices have been obtained: $S_x^T = 0.432$ and $S_y^T = 0.777$. It is apparent by qualitative considerations that the y position has more influence than the x position. The Sobol' indices confirm this aspect by providing a quantitative information.

An important thing to notice is the high value for the LOO, with almost 20%. This can be explained by the fact that $EI_{\max}$ is not a regular scalar output but the maximum of a list of different values. For two different sampled positions for the human body, the maximum of the list $\left(\{EI^i, \forall i \text{ tissue}\}\right)$ can be obtained for two different tissue types. Yet, this consistency is sufficient enough to draw tendencies on the safety of the WPT system regarding the position of the human body.

Finally, considering the mesh size (200 × 200) of the color map displayed in Fig. 4, a classical analysis would have required 40000 calls of the computational model instead of only $n_{samples} = 35$ for the training of our metamodel. On an Intel Core i7-10610U, 1.80 GHz, 8 GB of RAM, one datapoint takes 71 s. As the computation time of the metamodel itself and the grid plotting time can be negligible regarding the induced E-fields computations, a classical analysis would take around 33 days, while our algorithm took only 42 min to build an accurate predictor. Therefore, even if the system considered here is completely safe, the developed methodology is of great interest to reduce computation time of exposure problems.

IV. EXPOSURE TO AN MFDC SPOT WELDING GUN

The previously developed dosimetric protocol has been extended to an MFDC welding gun (see Fig. 5a) in order to investigate the human exposure of resistance spot welding processes (see Fig. 5b). This resistance welding process consists in heating the metal at the joint using a high current pulse. Thus, the levels of stray magnetic field generated by this device are extremely high compared to WPT systems. Moreover, because the generated magnetic field comes from a current pulse, the device does not work at a fixed frequency unlike the WPT3/Z3 system studied earlier. Therefore, the challenge is to properly assess the human exposure of the gun while taking into account all the frequencies in the pulse spectrum, indeed, the reference levels are dependent on the body area but also on the input frequency.

A. SIMPLE MODEL FOR A WELDING GUN

The welding pulse taken into account in the analysis has been measured during our previous works [10], [32]. The considered current pulse (shown in blue in Fig. 6a) is a rectangular pulse with 5 ms of raising time, an amplitude of 15 kA and a weld time of 200 ms. As observed on its spectrum (displayed in Fig. 6b), many harmonics are irrelevant in the analysis and are making it extremely dense, thus, difficult to work with for the analysis. Therefore, all the harmonics

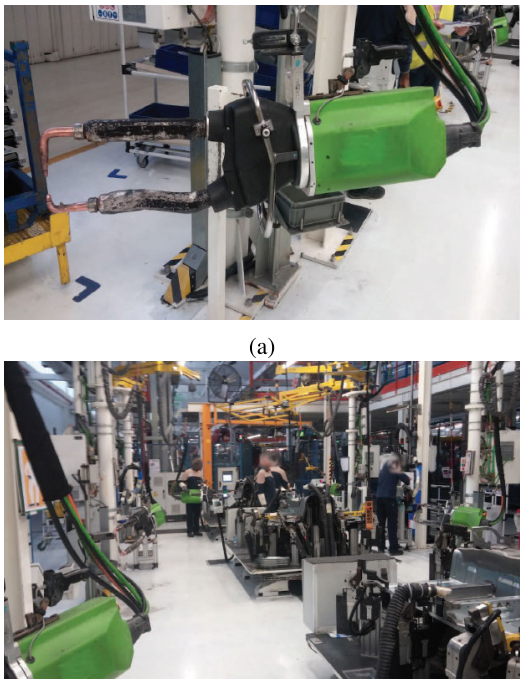

FIGURE 5. An MFDC welding gun (a) used to perform welding operations in a working area (b), taken from [31].

below 1% of the fundamental (black line in Fig. 6b) have been considered negligible and removed from the spectrum. The resulting spectrum is displayed in red in Fig. 6b, with the corresponding signal computed with an inverse fast Fourier transform displayed in Fig. 6a in red. This signal will be the one considered in this analysis.

The gun body along with the MF transformer is considered shielded [32]. Therefore, the welding gun has been modelled in Sim4Life as a simple rectangular current loop (0.5 m × 0.2 m, in blue in Fig. 7), as made in [10]. The gun is simulated at a fixed height ($z = 1.25$ m in the different simulations). At a given frequency, the magnetic vector potential and the Magnetic Flux density can be computed using the built-in FDTD LF Magneto Static Vector Potential solver and then, the Duke's model is placed in the vicinity area considered as vacuum (see Fig. 7).

B. MULTI-FREQUENCY EXPOSURE FACTOR

Unlike a WPT system, the waveforms generated for MFDC welding guns are pulses, thus, producing non-sinusoidal fields. Therefore, the computation of the exposure index can be performed using the weighted peak method (WPM, [33]) as suggested by the ICNIRP [2]. For a given tissue i in the human body, EI^i must verify:

$$EI^i = \left| \sum_j \frac{E^i_{99^{\text{th}}}}{E^i_{lim}(f_j)} \cos(2\pi f_j t + \theta_j + \varphi_j) \right| < 1 \qquad (6)$$

where $(E^i_{99^{\text{th}}}, \theta)$ is the 99$^{\text{th}}$ percentile of the induced E-field RMS value and its phase, (E^i_{lim}, φ) the corresponding

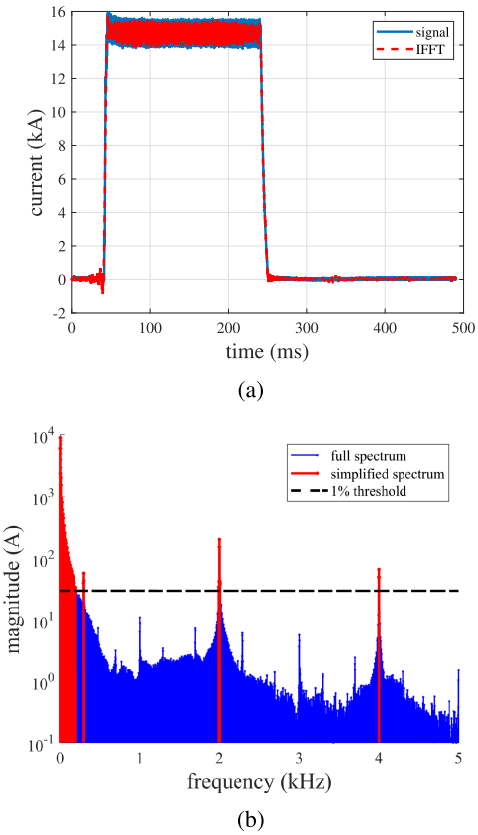

FIGURE 6. Real welding current pulse measured at PoliTO (in blue) with the simplified pulse considered in our simulation (in red) (a), original and simplified spectrum of the measured current pulse with the black line at 1% of the fundamental (b).

reference level and phase at the given frequency f_j. The WPM behaves like a low-pass filter whose magnitude is $1/E^i_{lim}$ and the phase is φ_j at the given frequency f_j [34]. These parameters are defined in the ICNIRP 2010 guidelines [2]. The characteristics of the filter for a central nervous system (CNS) tissue of the head in the case of occupational and general public exposure are displayed in Fig. 8.

Similarly as the previous analysis, for assessing the safety of the given position for the operator of the welding gun, the chosen exposure criteria is the maximum among all exposure indices available: $EI_{\max} = \max\left(\{EI^i, \forall i \text{ tissue}\}\right)$.

C. FREQUENCY SCALING

In order to compute the total exposure index $EI_{\max}$ for a single position (x, y) of the human body around the welding gun, a lot of computation would be needed due to all the frequencies in the pulse spectrum and all the different tissues in the human body. Therefore, the goal is to simplify the electromagnetic problem in order to compute the dosimetric quantities only at a given frequency. At each position (x, y) investigated in the active learning algorithm, only one call of the Sim4Life model is made. The resulting dosimetry quantity can then be used to compute the total exposure index $EI_{\max}$ at this single position by post-processing.

The computation of the induced E-field in a given tissue i can be performed at a single frequency f: $\vec{E}^i(f)$. Then, this

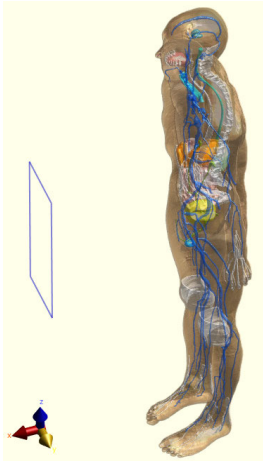

FIGURE 7. Duke's model for the operator facing the rectangular current loop (in blue) from the MFDC spot welding gun.

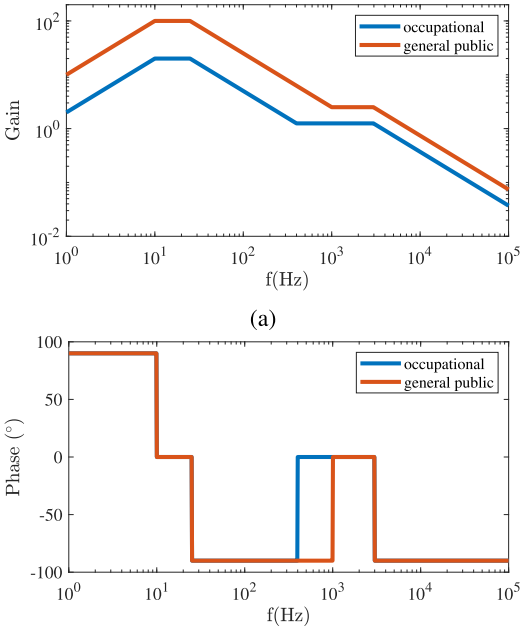

FIGURE 8. Gain (a) and phase (b) of the WPM filter for CNS tissue of the head in the case of an occupational exposure (blue) and general exposure (red) for the induced *E*-field.

result can be transposed to any frequency using frequency scaling with the quasi-static approximation [35]:

$$\forall f', \overrightarrow{E}^{\,i}(f') = \left(\frac{f'}{f}\right)\left(\frac{\sigma + j\omega\varepsilon}{\sigma' + j\omega'\varepsilon'}\right)\left(\frac{I'}{I}\right)\overrightarrow{E}^{\,i}(f) \quad (7)$$

with (σ, σ') and $(\varepsilon, \varepsilon')$ the conductivity and permittivity of tissue i at the frequencies f and f', and I, I' the amplitude in the simplified spectrum of the current pulse at the angular frequencies $\omega = 2\pi f$ and $\omega' = 2\pi f'$. The quasi-static approximation is valid here as for $f_{\max} = 4\,\text{kHz}$, $\lambda \simeq 7.49 \times 10^5\,\text{m}$ which is huge compared to the size of the body. The variation of the dielectric properties regarding the frequency for all considered tissues have been computed using the values from the IT'IS database [17].

TABLE 4. Relevant tissues considered in our WPM analysis with the number of studies in the literature used to build the low frequency dielectric model in the IT'IS database [17].

Tissue	number of studies
Bone Marrow (Yellow)	25
Cerebellum	33
Brain (Grey Matter)	214
Brain (White Matter)	194
Fat	91
SAT (Subcutaneous Fat)	91
Skin (Dry)	7
Spinal Cord	60

D. CHOICE OF CRITICAL TISSUES

The frequency scaling is relying on the known variation of the dielectric properties $(\sigma^i, \varepsilon_r^i)$ against the frequency for all considered tissues. Unfortunately the frequency dependency of most tissue properties is not yet fully reliable for frequencies below 1 MHz. Thus, for the exposure assessment of the MFDC spot welding gun, the weighted peak method has only been applied to a handful of tissues. The chosen tissues are the ones among the IT'IS database with many studies conducted on it. Moreover, a second selection of critical tissues has been done, which are known in the literature to exceed exposure limits in the vicinity of MFDC welding guns [36]. This enables us to compute fewer dosimetric quantities and speeds up at the same time the complete computation of the metamodel by preventing to compute irrelevant data regarding the safety of the device. The chosen tissues with the number of samples used for building the dielectric model against the frequency are displayed in Table 4.

E. EXPOSURE FACTOR METAMODELING

The welding gun is considered at a stationary position throughout the analysis and the Duke's model is moved in a vicinity area behind the gun (see Fig. 9) along the x and y axis. The possible ranges of variations for the (x, y) position of the human body (center of the box surrounding the Duke's model) are $x \in [140\,\text{mm}, 640\,\text{mm}]$ and $y \in [-700\,\text{mm}, 700\,\text{mm}]$.

For a given position (x, y), the 99$^{\text{th}}$ percentile induced electric field is computed in each of the 8 considered tissues at a single frequency $f = 46.94\,\text{Hz}$. A datapoint for the metamodel is therefore the position (x, y) and the corresponding 8 by 1 vector for the induced E-fields. Thus, using the active learning metamodel algorithm, 8 different metamodels are computed for the 99$^{\text{th}}$ percentile induced electric field for every tissue type considered at the frequency f against the position of the human body. The resulting sensitivity analysis is displayed on Table 5.

The active learning metamodelling algorithm has been successful at building the various predictors for all considered tissues with only $n_{samples} = 28$. The resulting LOO values are not exceeding 10% apart from the metamodel for the skin at 11.5%. Therefore the resulting predictor for each tissue are consistent enough to be used for sensitivity analysis but

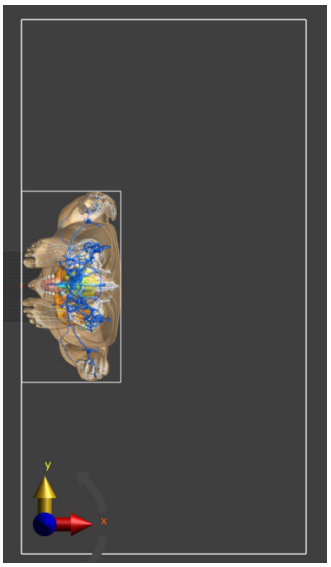

FIGURE 9. Vicinity area considered for the exposure problem behind the MFDC welding gun.

TABLE 5. Sensitivity analysis for the 99th percentile induced E-field in the relevant tissues considered in our WPM analysis against the position of the human body behind the welding gun ($n_{samples} = 28$, mean $LOO = 0.0545$).

Tissue	S_x^T	S_y^T	LOO
Bone Marrow (Yellow)	0.789	0.391	0.04790
Cerebellum	0.775	0.272	0.00930
Brain (Grey Matter)	0.918	0.151	0.00624
Brain (White Matter)	0.872	0.186	0.01140
Fat	0.683	0.478	0.09430
SAT (Subcutaneous Fat)	0.696	0.478	0.0695
Skin (Dry)	0.610	0.539	0.11500
Spinal Cord	0.907	0.190	0.08230

also exposure factor computations. As for the WPT structure, regarding the sensitivity analysis, the conclusion is similar with the x axis being the most important direction for most tissues while the y position being not negligible. Thus, the operator is safer at standing on the side of the gun instead of in front of it.

F. SAFETY AREA BEHIND THE GUN

For a given position (x, y) of the Duke's model, using the available consistent predictor on each of the 99th percentile induced E-field at f, with 7, the 99th percentile induced E-field can be computed at every frequency of the pulse spectrum. Then the weighted peak method (see section 6) can be applied to the 8 different tissues where 8 peaks $I^i_{WP} = \max(EI^i_{\max}, \forall t)$ can be detected. This leads to the definition of a safety area when analyzing $(x, y, \max(I^i_{WP}, \forall i))$ if all peaks do not exceed one.

The variations of $\max(I^i_{WP})$ behind the gun and the safety area where $\max(I^i_{WP}) < 1$ are displayed for occupational exposure in Fig. 10a. Considering our computation box (see Fig. 9), most of the vicinity area of the welding gun is safe for the operator. Close to the gun, the exposure index is

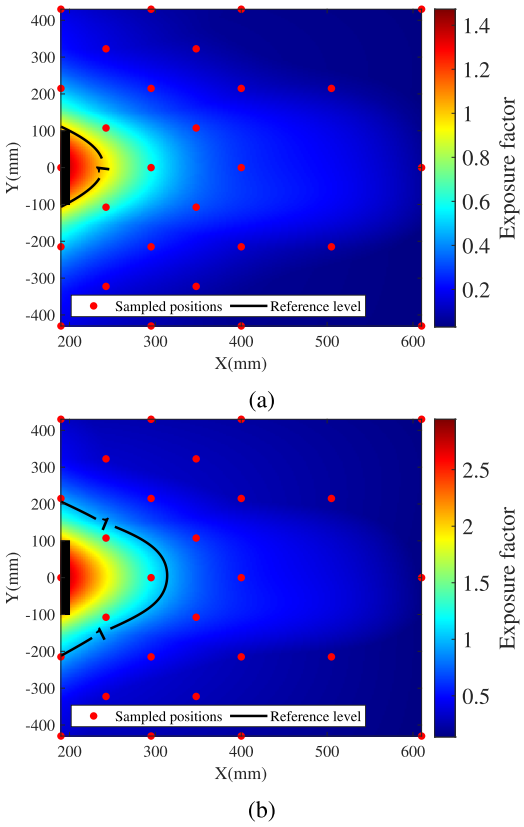

FIGURE 10. Variation of the exposure index and safety area ($\max(I^i_{WP}) < 1$) behind the MFDC welding gun for occupational exposure (a) and general public exposure (b).

exceeding 1, meaning the 99th percentile induced E-field is above the limit for at least one of the 8 tissue types considered. Therefore, the safety area on all sides is at least 250 mm behind the gun. From the industrial point of view, this safety area correlates the observation already made on existing operating devices in [31]. Indeed, in the case of general public exposure (see Fig. 10b), this system might be more dangerous. This time the safety area on all sides is at least 325 mm behind the gun. That is why some protections have been developed especially for the arms around the welding device.

G. DISCUSSION

These simulations are all based on the current pulse of Fig. 6 and the results provided here could be different for another pulse. This simulation has been performed in order to display the tendencies of such an high-power device and to show the use of the various methodologies coupled with a metamodelling process.

Again, considering the mesh size (200 × 200) for the various color maps displayed in Fig. 10 and 11, as for this system one datapoint takes around 3 min, a classical analysis would take around 84 days, while our algorithm took only 84 min to build an accurate predictor. Compared to the existing methodologies for the exposure assessment of MFDC welding guns cited earlier, our development brings a

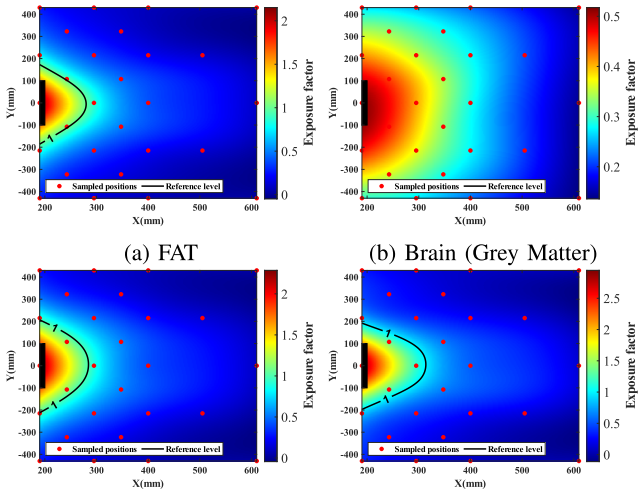

(a) FAT (b) Brain (Grey Matter)

(c) SAT (Subcutaneous Fat) (d) Skin (Dry)

FIGURE 11. Variation of the exposure factor and safety area ($I_{WP} < 1$) behind the MFDC welding gun for different tissues investigated in the case of general public exposure.

TABLE 6. Estimated gain in computation time for the two exposure analysis compared to brute-force analysis which requires 40000 samples.

Analysis	*LOO* (averaged)	brute-force analysis	computation metamodel	time reduction
WPT3/Z3 system	0.1945	33 days	35 samples in 42 min	99.91%
MFDC spot welding gun	0.0545	83 days	28 samples in 84 min	99.93%

great decrease in computation time for this complex system. Thanks to the reliable computed predictor, various mitigation solutions for the welding gun could be analyzed fastly along with the influence of various welding parameters such as the rising time of the pulse or the peak current [32].

Using the predictors available for the 8 different tissues previously considered, the same safety area analysis can be performed on each tissue separately to see which tissues are the most solicited during the welding process. The resulting safety areas for each tissue (for general public exposure) are displayed in Fig. 11. The critical tissues in our simulation are the skin along with the fat and subcutaneous fat as their safety area are the largest, while the other five tissues are perfectly safe during the magnetic pulse. These results could help in developing new protecting clothing or devices to reduce the exposure of specific tissues.

V. CONCLUSION

Our goal was here to demonstrate the usefulness of adaptive surrogate techniques and of metamodelling in general for complex electromagnetic problems in the case of human exposure. These analyses are more difficult to compute than classical problems as the magnetic field need to be computed in the first place then a voxel-based 3D human model can be placed within and the dosimetric analysis computed. Then, the results can be used to try out mitigation solutions or define safety area around high-power devices.

The algorithm has been first successful at estimating exposure around the simulated WPT3 (class Z3) from the Standard SAE J2954 on its worst case (maximum misalignment between coils). Even if the interest is of no use as the system is perfectly safe (the exposure index did not exceed 0.45), the methodology employed here can be of use for future exposure analysis around high-power systems. The combination of the quad-tree algorithm for samples with Sim4Life for datapoints computation on a provided *B*-field managed to provide a consistent predictor for the exposure regarding the position of a crouching posture (worst posture) around the working WPT device. Then, this dosimetric protocol has been extended to a system where the human exposure problem is more critical: MFDC welding guns, another high-power system. By using just a simple model (planar coil) for the gun with a magnetic current pulse, a multi-frequency metamodel for the exposure factor on some critical tissues has been obtained for any relative distance of the human body behind the gun. Using the corresponding predictor, some compliance safety areas around the device have been defined using the WPM for 8 particular tissues.

Our methodology based on metamodelling has been proven quite useful for fast and reliable computation in terms of exposure assessment. It proposed an alternative to existing time reducing solutions mentioned earlier. Compared to a classical brute-force method, the gain in computation time is over 99.9% for both analysis as shown in table 6. Even if some better sampling methods could be use for a classical analysis, our methodology would still require far less calls of the heavy computational model. The main advantages of using our metamodelling algorithms instead of other numerical methods is first its overall simplicity in its setup: the model definition itself is needed along with the input parameter space, once a consistent metamodel has been built, no additional computations are required. Then, the resulting predictor can be used easily for various other applications such as optimisation or global sensitivity analysis. But using such an adaptive algorithm brings also a potential drawback as a tweak of the active learning parameters might be needed if different high-power systems, in terms of exposure scenario or model complexity, are to be studied. This would take several roll of the algorithm to compute a consistent metamodel, thus increasing the global computation time while still being lower than classical numerical methods.

REFERENCES

[1] A. Hirata, Y. Diao, T. Onishi, K. Sasaki, S. Ahn, D. Colombi, V. De Santis, I. Laakso, L. Giaccone, W. Joseph, E. A. Rashed, W. Kainz, and J. Chen, "Assessment of human exposure to electromagnetic fields: Review and future directions," *IEEE Trans. Electromagn. Compat.*, vol. 63, no. 5, pp. 1619–1630, Oct. 2021.

[2] International Commission on Non-Ionizing Radiation Protection, "Guidelines for limiting exposure to time-varying electric and magnetic fields (1 Hz to 100 kHz)," *Health Phys.*, vol. 99, no. 6, pp. 818–836, 2010.

[3] W. H. Bailey, R. Bodemann, J. Bushberg, C. Chou, R. Cleveland, A. Faraone, K. R. Foster, K. E. Gettman, K. Graf, and T. Har-Rington, "Synopsis of IEEE Std C95. 1–2019 'IEEE standard for safety levels with respect to human exposure to electric,'" *IEEE Access*, vol. 7, pp. 171346–171356, 2019.

[4] M.-C. Gosselin, E. Neufeld, H. Moser, E. Huber, S. Farcito, L. Gerber, M. Jedensjö, I. Hilber, F. D. Gennaro, B. Lloyd, E. Cherubini, D. Szczerba, W. Kainz, and N. Kuster, "Development of a new generation of high-resolution anatomical models for medical device evaluation: The virtual population 3.0," *Phys. Med. Biol.*, vol. 59, no. 18, pp. 5287–5303, Sep. 2014.
[5] E. Yavolovskaya, G. Chiqovani, G. Gabriadze, S. Iosava, L. Svanidze, B. Willmann, and R. Jobava, "Simulation of human exposure to electromagnetic fields of inductive wireless power transfer systems in the frequency range from 1 Hz to 30 MHz," in *Proc. Int. Symp. Electromagn. Compat.*, Sep. 2016, pp. 491–496.
[6] M. Zang, M. Clemens, C. Cimala, J. Streckert, and B. Schmuelling, "Simulation of inductive power transfer systems exposing a human body with two-step scaled-frequency FDTD methods," *IEEE Trans. Magn.*, vol. 53, no. 6, pp. 1–4, Jun. 2017.
[7] G. Ferraris, "Human exposure to low-frequency magnetic field: New methodologies for numerical dosimetry," Ph.D. dissertation, Dept. Energy, Politecnico di Torino, Turin, Italy, 2022. [Online]. Available: http://hdl.handle.net/11583/2968460
[8] J. Chakarothai, K. Wake, T. Arima, S. Watanabe, and T. Uno, "Exposure evaluation of an actual wireless power transfer system for an electric vehicle with near-field measurement," *IEEE Trans. Microw. Theory Techn.*, vol. 66, no. 3, pp. 1543–1552, Mar. 2018.
[9] T. W. Dawson, K. Caputa, and M. A. Stuchly, "Electric fields induced in humans and rodents by 60 Hz magnetic fields," *Phys. Med. Biol.*, vol. 47, no. 14, pp. 2561–2568, Jul. 2002.
[10] A. Canova, F. Freschi, L. Giaccone, and M. Manca, "A simplified procedure for the exposure to the magnetic field produced by resistance spot welding guns," *IEEE Trans. Magn.*, vol. 52, no. 3, pp. 1–4, Mar. 2016.
[11] P. Kersaudy, B. Sudret, N. Varsier, O. Picon, and J. Wiart, "A new surrogate modeling technique combining Kriging and polynomial chaos expansions—Application to uncertainty analysis in computational dosimetry," *J. Comput. Phys.*, vol. 286, pp. 103–117, Apr. 2015.
[12] P. Lagouanelle, O. Bottauscio, L. Pichon, and M. Zucca, "Impact of parameters variability on the level of human exposure due to inductive power transfer," *IEEE Trans. Magn.*, vol. 57, no. 6, pp. 1–4, Jun. 2021.
[13] T. W. Dawson and M. A. Stuchly, "High-resolution organ dosimetry for human exposure to low-frequency magnetic fields," *IEEE Trans. Magn.*, vol. 34, no. 3, pp. 708–718, May 1998.
[14] F. Freschi, L. Giaccone, and M. Repetto, "Algebraic formulation of nonlinear surface impedance boundary condition coupled with BEM for unstructured meshes," *Eng. Anal. Boundary Elements*, vol. 88, pp. 104–114, Mar. 2018.
[15] T. W. Dawson and M. A. Stuchly, "Analytic validation of a three-dimensional scalar-potential finite-difference code for low-frequency magnetic induction," *Appl. Comput. Electromagn. Soc. J.*, vol. 11, pp. 72–81, Jan. 1996.
[16] M. Zang, C. Cimala, M. Clemens, J. Dutiné, T. Timm, and B. Schmuelling, "A co-simulation scalar-potential finite difference method for the numerical analysis of human exposure to magneto-quasi-static fields," *IEEE Trans. Magn.*, vol. 53, no. 6, pp. 1–4, Jun. 2017.
[17] P. Hasgall, F. Di Gennaro, C. Baumgartner, E. Neufeld, B. Lloyd, M. Gosselin, D. Payne, A. Klingenböck, and N. Kuster, "It database for thermal and electromagnetic parameters of biological tissues version 4.1," Version 4.1, Feb. 2022, doi: 10.13099/VIP21000-04-1.
[18] R. Schobi, B. Sudret, and J. Wiart, "Polynomial-chaos-based Kriging," *Int. J. Uncertainty Quantification*, vol. 5, no. 2, pp. 171–193, 2015.
[19] P. Lagouanelle, "Metamodel-based methodology for fast prediction of human exposure due to high power systems," Ph.D. dissertation, Dipartimento Energia, Politecnico di Torino, Turin, Italy Group Elect. Eng.-Paris (GeePs), UMR CNRS 8507, CentraleSupélec, Université Paris-Saclay, Sorbonne Université, Gif-sur-Yvette, France, 2023. [Online]. Available: http://www.theses.fr/2023UPAST029
[20] R. A. Finkel and J. L. Bentley, "Quad trees a data structure for retrieval on composite keys," *Acta Inf.*, vol. 4, no. 1, pp. 1–9, 1974.
[21] P. Lagouanelle, F. Freschi, and L. Pichon, "Adaptive sampling for fast and accurate metamodel-based sensitivity analysis of complex electromagnetic problems," *IEEE Trans. Electromagn. Compat.*, vol. 65, no. 6, pp. 1820–1828, Dec. 2023.
[22] R. Teixeira, B. Martinez-Pastor, M. Nogal, and A. O'Connor, "Reliability analysis using a multi-metamodel complement-basis approach," *Rel. Eng. Syst. Saf.*, vol. 205, Jan. 2021, Art. no. 107248.
[23] I. M. Sobol, "Sensitivity analysis for non-linear mathematical models," *Math. Model. Comput. Exp.*, vol. 1, pp. 407–414, Jan. 1993.
[24] B. Sudret, "Uncertainty propagation and sensitivity analysis in mechanical models—Contributions to structural reliability and stochastic spectral methods," Habilitatio Diriger Des Recherches, Univ. laise PASCAL, Clermont-Ferrand, France, Tech. Rep., 147, 2007, p. 53.
[25] *Wireless Power Transfer for Light-Duty Plug-in/Electric Vehicles and Alignment Methodology*, Standard J2954, 2016.
[26] T. Shimamoto, I. Laakso, and A. Hirata, "In-situ electric field in human body model in different postures for wireless power transfer system in an electrical vehicle," *Phys. Med. Biol.*, vol. 60, no. 1, pp. 163–173, Jan. 2015.
[27] V. De Santis, L. Giaccone, and F. Freschi, "Influence of posture and coil position on the safety of a WPT system while recharging a compact EV," *Energies*, vol. 14, no. 21, p. 7248, Nov. 2021.
[28] I. Laakso and A. Hirata, "Reducing the staircasing error in computational dosimetry of low-frequency electromagnetic fields," *Phys. Med. Biol.*, vol. 57, no. 4, pp. 25–34, Feb. 2012.
[29] J. Gomez-Tames, I. Laakso, Y. Haba, A. Hirata, D. Poljak, and K. Yamazaki, "Computational artifacts of the in situ electric field in anatomical models exposed to low-frequency magnetic field," *IEEE Trans. Electromagn. Compat.*, vol. 60, no. 3, pp. 589–597, Jun. 2018.
[30] A. Arduino, O. Bottauscio, M. Chiampi, L. Giaccone, I. Liorni, N. Kuster, L. Zilberti, and M. Zucca, "Accuracy assessment of numerical dosimetry for the evaluation of human exposure to electric vehicle inductive charging systems," *IEEE Trans. Electromagn. Compat.*, vol. 62, no. 5, pp. 1939–1950, Oct. 2020.
[31] A. Canova, F. Freschi, and L. Giaccone, "How safe are spot welding guns to use: An analysis of occupational exposure to their magnetic field," *IEEE Ind. Appl. Mag.*, vol. 24, no. 3, pp. 39–47, May 2018.
[32] L. Giaccone, V. Cirimele, and A. Canova, "Mitigation solutions for the magnetic field produced by MFDC spot welding guns," *IEEE Trans. Electromagn. Compat.*, vol. 62, no. 1, pp. 83–92, Feb. 2020.
[33] K. Jokela, "Restricting exposure to pulsed and broadband magnetic fields," *Health Phys.*, vol. 79, no. 4, pp. 373–388, Oct. 2000.
[34] L. Giaccone, "Uncertainty quantification in the assessment of human exposure to pulsed or multi-frequency fields," *Phys. Med. Biol.*, vol. 68, no. 9, May 2023, Art. no. 095001.
[35] A. W. Guy, S. Davidow, G. Yang, and C. Chou, "Determination of electric current distributions in animals and humans exposed to a uniform 60-Hz high-intensity electric field," *Bioelectromagnetics*, vol. 3, no. 1, pp. 47–71, Jan. 1982.
[36] L. Giaccone, "Compliance of non-sinusoidal or pulsed magnetic fields generated by industrial sources with reference to human exposure guidelines," in *Proc. Int. Symp. Electromagn. Compat.*, Sep. 2020, pp. 1–6.

PAUL LAGOUANELLE was born in Toulouse, France, in 1995. He received the master's degree in physics from École Normale Supérieure de Cachan (now ENS Paris-Saclay), in 2019. He is currently pursuing the joint Ph.D. degree with the Group of Electrical Engineering and Politecnico di Torino, Italy, with a focus on surrogate modeling methods applied to human exposure assessment for high-power systems. He has completed the master's thesis with the Group of Electrical Engineering.

His research and scientific interests include numerical modeling for electromagnetics and electromagnetic compatibility.

FABIO FRESCHI (Senior Member, IEEE) received the M.Sc. (summa cum laude) and Ph.D. degrees in electrical engineering from Politecnico di Torino, in 2002 and 2006, respectively.

In 2006, he was a Visiting Researcher with the Technical University of Graz, Graz, Austria. He was appointed as an Adjunct Senior Fellow with The University of Queensland, Australia, from 2014 to 2020. He is currently a Full Professor in fundamentals of electrical engineering with Politecnico di Torino. His research and scientific interests include numerical modeling and computation of electromagnetic and coupled fields using differential, integral, and hybrid techniques. He coauthored more than 150 conference and journal papers in these fields.

Dr. Freschi was a recipient of several international awards issued by IEEE. Since 2022, he has been included in the World's 2% Top Scientist list prepared by Stanford University and Elsevier. He is an Associate Editor of IEEE INDUSTRY APPLICATIONS SOCIETY and he serves as a referee of many international journals in the field of numerical electromagnetics, optimization, and operational research.

LIONEL PICHON received the Dip.-Eng. degree from École Supérieure d'Ingénieurs en Electrotechnique et Electronique, in 1984, and the Ph.D. degree in electrical engineering from Laboratoire de génie électrique de Paris, in 1989.

He got a position with Centre National de la Recherche Scientifique (CNRS), in 1989. He is currently a Directeur de recherche (a Senior Research Scientist) with the Group of Electrical Engineering–Paris (GeePs), a laboratory belonging to four institutions: CNRS, CentraleSupélec, Université Paris-Saclay, and Sorbonne Université. He is the author or coauthor of more than 130 journal articles in peer-reviewed journals. His research interests include computational electromagnetics, electromagnetic compatibility, and wireless power transfer. He is an Associate Editor of *The European Physical Journal Applied Physics* (EPJ AP). He is serving as a reviewer for several scientific international journals.

LUCA GIACCONE (Senior Member, IEEE) was born in Cuneo, Italy, in 1980. He received the Laurea and Ph.D. degrees in electrical engineering from Politecnico di Torino, Turin, Italy, in 2005 and 2010, respectively.

Since 2017, he has been an Associate Professor with Dipartimento Energia "G. Ferraris," Politecnico di Torino. In 2020, he was appointed as a member of the ICNIRP Scientific Expert Group (SEG). He works on several areas of electrical engineering: optimization, modeling of complex energy systems, computation of electromagnetic and thermal fields, energy scavenging, magnetic field mitigation, EMF dosimetry, and compliance of LF pulsed magnetic field sources.

Dr. Giaccone has been a member of the IEEE International Committee on Electromagnetic Safety—Technical Committee 95-SC6-dosimetry modeling, since 2015. Since September 2017, he has been a member of the National Italian Committee CEI-106 dealing with human exposure to electromagnetic fields.

Open Access funding provided by 'Politecnico di Torino' within the CRUI CARE Agreement